Hindawi Publishing Corporation
Journal of Nanomaterials
Volume 2014, Article ID 670849, 6 pages
http://dx.doi.org/10.1155/2014/670849

Research Article

In Situ Study of Thermal Stability of Copper Oxide Nanowires at Anaerobic Environment

Lihui Zhang,[1] Qiong Feng,[2] Anmin Nie,[2] Jiabin Liu,[1,3] Hongtao Wang,[2] and Youtong Fang[1]

[1] *College of Electrical Engineering, Zhejiang University, Hangzhou 310027, China*
[2] *Institute of Applied Mechanics, Zhejiang University, Hangzhou 310027, China*
[3] *Department of Materials Science and Engineering, Zhejiang University, Hangzhou 310027, China*

Correspondence should be addressed to Jiabin Liu; liujiabin@zju.edu.cn and Hongtao Wang; htw@zju.edu.cn

Received 27 May 2014; Accepted 24 June 2014; Published 24 July 2014

Academic Editor: Vladimir Sivakov

Many metal oxides with promising electrochemical properties were developed recently. Before those metal oxides realize the use as an anode in lithium ion batteries, their thermal stability at anaerobic environment inside batteries should be clearly understood for safety. In this study, copper oxide nanowires were investigated as an example. Several kinds of *in situ* experiment methods including *in situ* optical microscopy, *in situ* Raman spectrum, and *in situ* transmission electron microscopy were adopted to fully investigate their thermal stability at anaerobic environment. Copper oxide nanowires begin to transform as copper(I) oxide at about 250°C and finish at about 400°C. The phase transformation proceeds with a homogeneous nucleation.

1. Introduction

Energy issues become more and more important today than those at any time in the past. Lithium ion batteries (LIBs), as one of the most promising technologies, have obtained high attentions in both industry and science societies. Important advances have been made for further improving the battery properties recently, such as the developments of Li-O_2 and Li-S batteries, Na-ion batteries, and double-walled silicon nanotube batteries [1–6].

The anode material is one of the most important components in LIBs. Graphite was the first commercialized anode material due to its good cycle performance. However, relatively low theoretical capacity (~372 mAh/g) of graphite stimulated the study of other high energy density anode materials [7]. A number of anode materials, such as aluminum [8, 9], tin [10, 11], germanium [12, 13], and silicon [14, 15] were developed over the past few years [6, 7, 16–20].

Metal oxides, expected to be important anode materials in the future, have high theoretical capacity. SnO_2, Co_3O_4, RuO_2, and TiO_2 anodes [18, 21–26] have several advantages compared to others. The research team headed by Huang et al. revealed the charge-discharge lithium mechanism of metal oxide nanowires by *in situ* lithiation-delithiation in transmission electron microscopy (TEM) [27, 28]. Those researchers have greatly enhanced our understanding of the charge-discharge lithium mechanism of metal oxides and promoted the development of science and technology.

Metal oxides have high thermal stability in the oxygen environment. However whether they have high thermal stability at anaerobic environment in LIBs is still an open question. The accidents of "Boeing 787s" overheated batteries and "Sony" notebooks remind us that the thermal problems should never be an afterthought or dealt with lightly. The temperature in the batteries would significantly increase when the batteries are working at high current density. Some local areas may reach a rather high temperature due to the complicated and inhomogeneous microstructure of the anodes. The situation would be more significant for the Na/S and Na/$NiCl_2$ systems operating at higher temperatures (300–350°C) [29]. However, it is nearly a fresh area for the research on thermal stability of metal oxides in such a high temperature anaerobic environment.

Copper oxide nanomaterials have attracted great attentions and have demonstrated significant performances as anode materials [30–32]. It was reported that the capacity of the attenuation was less than 10% after 70 cycles and the cyclic capacity maintained at 400 mAh/g when using copper oxide

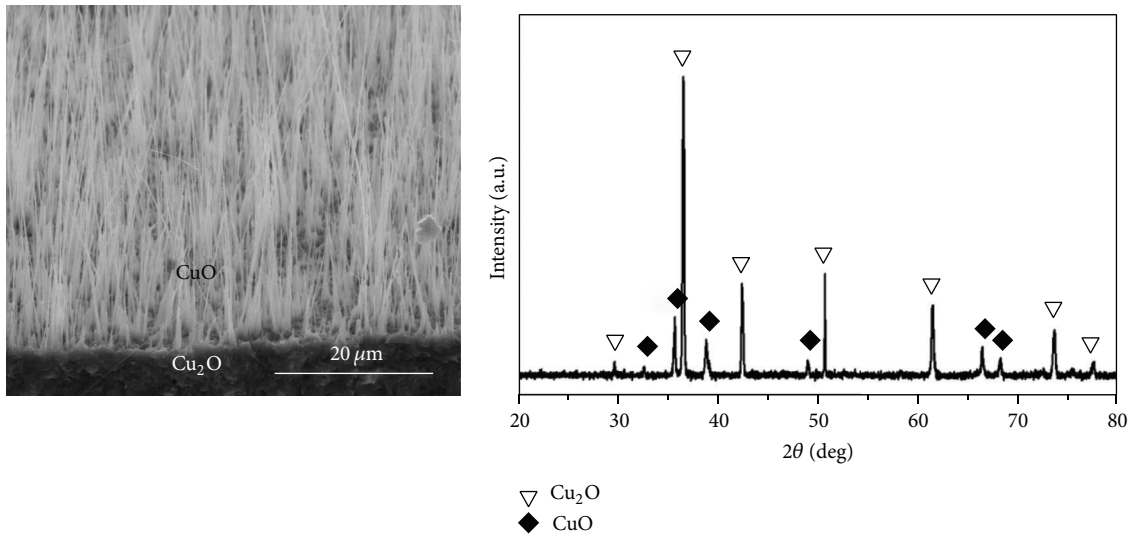

Figure 1: (a) SEM image of Cu foil oxide layer and (b) XRD pattern of Cu foil oxide layer.

nanowires as anodes [33]. Further improvement has been obtained that the cyclic capacity of copper oxide film could remain at 608 mAh/g with a current density of 100 mA/g after 275 cycles, which reached 90% of the theoretical capacity [34–37].

In this study, copper oxide nanowires were investigated as an example. Several *in situ* tests were adopted to explore the thermal stability of copper oxide nanowires at anaerobic environment directly. *In situ* optical microscopy, *in situ* Raman, and *in situ* TEM were carried out to study both the morphology and structure evolutions during *in situ* heating.

2. Materials and Methods

Cu foils (99.9% purity, Alfa Aesar Company) with a thickness of 25 μm were cleaned in an aqueous 1.0 mol/L HCl solution for 5~10 s, followed by repeated 2-3 times rinsing with deionized water. Cu foils were dried under N_2 gas flow, then placed in a rapid thermal processing system furnace (JET FIRST-200), and then heated to 500°C for 5 h in air ambient with a heating rate of 40°C/s.

The crystal structure of copper oxide was analyzed by X-ray diffraction (XRD, X'Pert PRO) with Cu-Kα radiation from 10° to 90°. The microstructure of the copper oxides was observed by scanning electron microscope (SEM, Hitachi S3700) and TEM (FEI F30). Some copper oxide nanowires were heated to a maximum temperature of 400°C with nitrogen atmosphere protection. The morphology change of the copper oxide nanowires was *in situ* observed under the optical microscope equipped in the Raman test system and the structure change of the copper oxide nanowires was *in situ* analyzed by Raman test during heating. The Raman spectra were recorded by using a LabRamHRUV instrument equipped with a 532 nm laser excitation. The microstructure change of the copper nanowires was *in situ* investigated in the TEM equipped with an *in situ* heating holder (Gatan 652).

3. Results and Discussion

High-density copper oxide nanowires are obtained when copper foils were oxidized in air ambient at 500°C for 5 h (Figure 1(a)). The average diameter of the nanowires is about 65 nm and the length of the nanowires is up to 20 μm. XRD pattern of the sample in Figure 1(a) indicates the coexistence of CuO phase of monoclinic structure (JCPDS80-1917) and Cu_2O phase of cubic structure (JCPDS78-2076) in the oxide layer (Figure 1(b)). The majority phase is the Cu_2O, which is in well accordance with previous studies [38]. Copper is always first oxidized into the Cu_2O phase and the subsequent formation of CuO phase would be very slow due to the cover of Cu_2O layer.

Figure 2(a) shows the TEM image of an individual nanowire with a diameter of about 60 nm. There is an interface obviously in the middle of nanowire which divides the nanowire into two planes along the longitudinal axis. The interface is confirmed to be twin boundary by select area electron diffraction (SAED) pattern analysis as shown in Figure 2(b). The nanowire is confirmed to be CuO nanowire by measuring the distance and angle of the diffraction spots in the SAED pattern. The SAED pattern corresponds to the two sets of lattice. One set diffraction spot of lattice is observed along the [110] direction while the other is observed along $[1\bar{1}0]$. High resolution TEM image clearly shows that the twin boundary is parallel with the (001) plane in Figure 2(c).

The morphology changes of the CuO nanowire at different temperatures at anaerobic environment were investigated by *in situ* heating an individual CuO nanowire with nitrogen atmosphere protection under an optical microscope. CuO nanowire has no obvious change when temperature is below 250°C (Figure 3(a)). When heating temperature reaches 300°C, some changes occur as pointed by the arrow in Figure 3(b). More changes appear as the temperature increases to 350°C (Figure 3(c)). Almost the entire nanowire

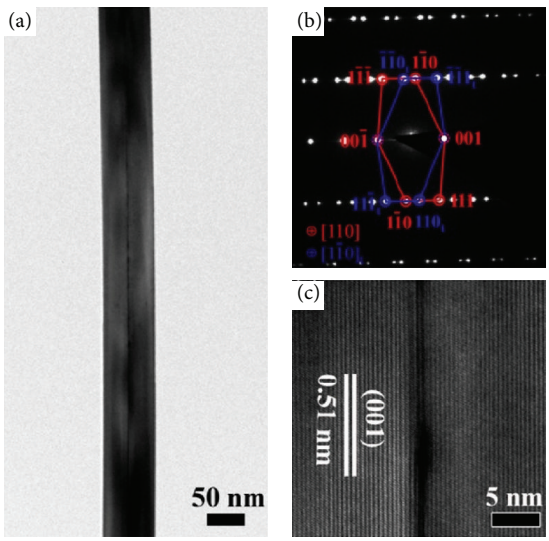

Figure 2: (a) TEM image of an individual CuO nanowire, (b) SAED pattern of the single nanowire, and (c) corresponding high resolution TEM image.

changes when the temperature increases to 400°C. The morphology changes of the nanowire indicate that there should be some transformation of the structure of CuO phase during the *in situ* heating process with a homogeneous nucleation behavior.

To analyze the structure change of the CuO nanowire during *in situ* heating process, *in situ* Raman test was carried out for the CuO nanowire heated at the same temperatures with nitrogen atmosphere protection (Figure 4). There are three Raman peaks at 296 cm^{-1}, 345 cm^{-1}, and 630 cm^{-1} for the test nanowire from 25°C to 250°C, which correspond to the A_g, B_{1g}, and B_{2g} modes [39] of CuO phase, respectively. When heating temperature reaches 300°C, two small new Raman peaks emerge at 154 cm^{-1} and 218 cm^{-1}, which consists with the Raman peaks of Cu_2O phase [40]. When the temperature continuously increases to 350°C and 400°C, the former three Raman peaks of CuO phase almost disappear and the two Raman peaks of Cu_2O phase enhance. Combining the *in situ* optical observation with Raman test results, it is reasonable to deduce that CuO phase should be transformed into Cu_2O with the increase in temperature under nitrogen atmosphere. The phase transformation begins at about 300°C and finishes at about 350°C.

For further study of the thermal stability of CuO nanowires, *in-situ* TEM heating experiments of CuO nanowires were carried out in vacuum of 10^{-6} Pa with heating holder. TEM images and corresponding SAED patterns of the *in situ* heated CuO nanowire are shown in Figure 5. There is no obvious change of morphology or SAED patterns of the CuO nanowire at temperatures below 200°C. The CuO nanowire is coated by a layer of amorphous carbon due to the heating and deposition effect in TEM. As the temperature increases to 250°C, some changes of CuO NW from the SAED patterns are noticed as pointed by arrows in Figure 5. At the same time, some slight new diffraction spots form as

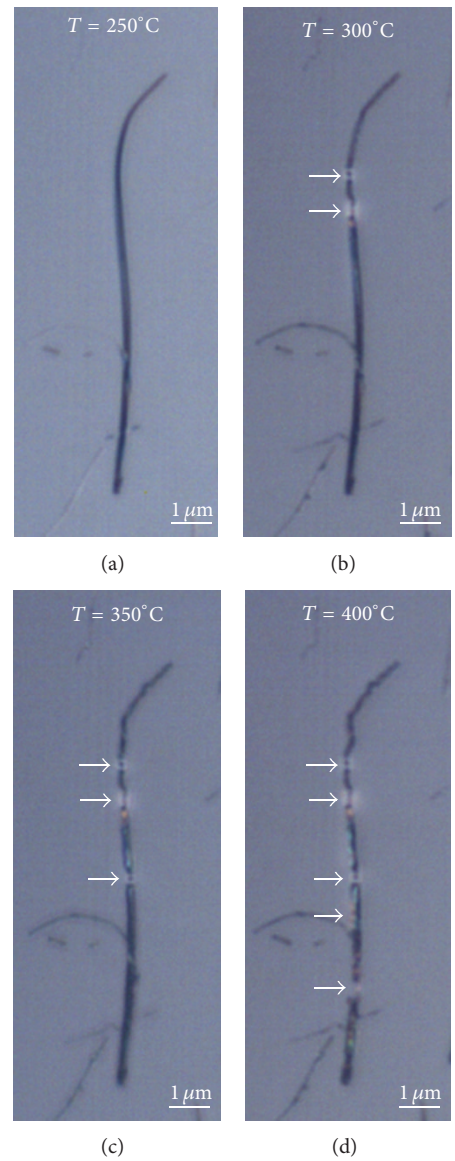

Figure 3: Optical microscopy images of the CuO nanowire *in situ* heated at different temperatures with nitrogen atmosphere protection (a) 250°C, (b) 300°C, (c) 350°C, and (d) 400°C.

indicated by arrows in the SAED patterns. Further increasing the temperature to 300°C and 350°C results in more obvious changes of the nanowire morphology and more new diffraction spots. When the temperature reaches 400°C, the original [110]CuO diffraction spots nearly disappear and the individual CuO nanowire is transformed into plenty of Cu_2O nanograins with a homogeneous nucleation mode. The new generated diffraction spots are well consistent with the SAED pattern of Cu_2O along the $[\bar{1}11]$ zone axis. The new spots which emerged at 250°C, 300°C, and 350°C are determined to belong to the SAED patterns of $[\bar{1}11]_{Cu_2O}$ by carefully analyzing and comparing the SAED patterns in Figure 5. The *in situ* TEM results agree well with the results of *in situ* optical microscope observation and *in situ* Raman test. The start phase transformation temperature detected in *in situ* TEM is

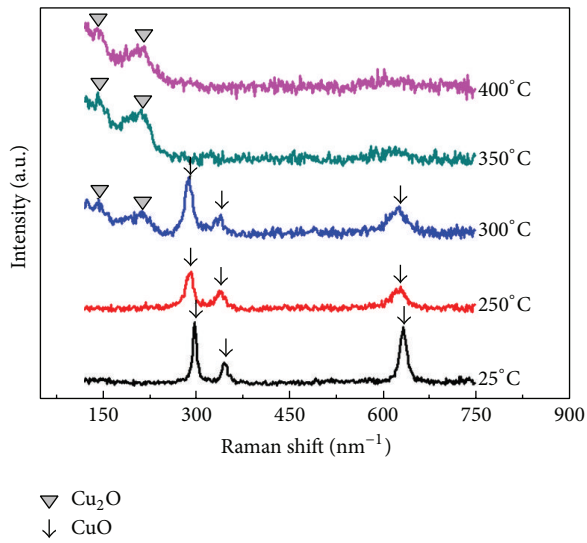

Figure 4: *In situ* Raman spectra of the CuO nanowire heated at different temperatures with nitrogen atmosphere protection.

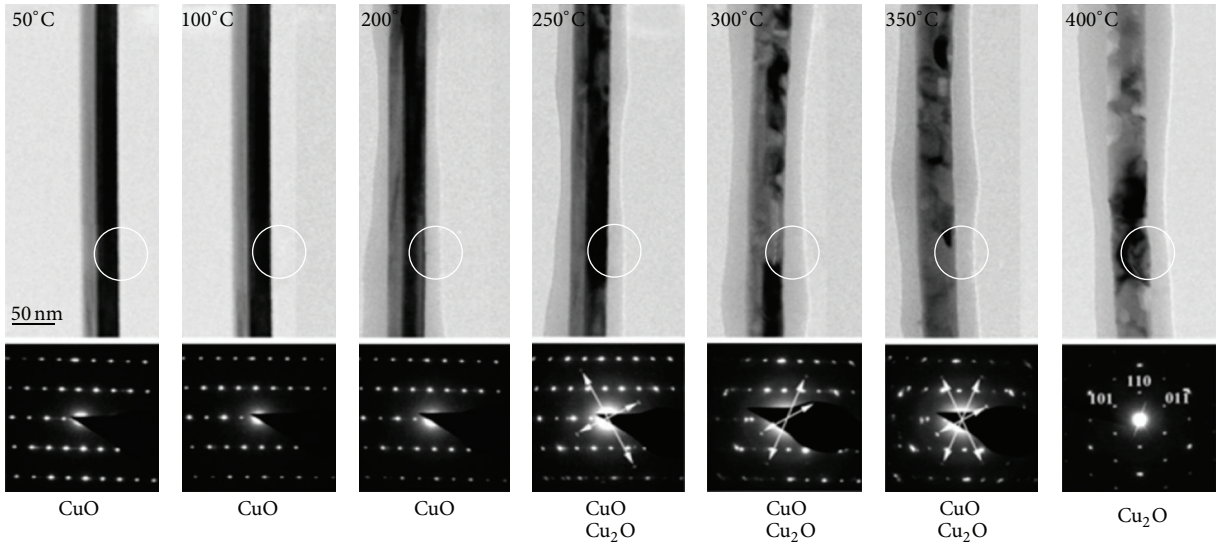

Figure 5: TEM images and SAED patterns corresponding to the white circle of an individual CuO nanowire *in situ* heated to different temperatures.

about 250°C while the temperature is about 300°C detected by *in situ* optical microscope and *in situ* Raman spectrum. The minor deviation of the start temperature should be attributed to the high resolution of the TEM technology. The above results are consistent well with the phase diagram determining the boundaries of temperature and oxygen pressure for maintaining the stability of Cu, Cu_2O, and CuO by Rakhshani [41]. It was believed that the CuO phase could be stabilized until 300°C at a very low oxygen pressure. In this study the phase transformation of CuO to Cu_2O begins at 250°C. The reason may be due to the nanoscale effect, which commonly decreases the melting temperature and phase transformation temperature as frequently reported in other nanomaterials [42–46]. Considering that the electrical resistivity of Cu_2O is three orders higher than that of CuO [41], the intrinsic resistivity of the LIBs would be greatly enhanced once some of CuO phase transformed into Cu_2O phase when the CuO is used as cathode. As a result, overheating or even explosion may be triggered when such LIBs are charged.

4. Conclusions

In this study, copper oxide nanowires were grown by a simple thermal oxide method. The average diameter of nanowires is 65 nm and the length is up to 20 μm. *In situ* Raman and optical microscope tests reveal that copper oxide nanowires gradually change into copper(I) oxide particles during *in situ* heating at anaerobic environment. *In situ* TEM test

further confirms that copper oxide begins to transform into copper(I) oxide at 250°C and nearly finish at 400°C with a homogeneous nucleation behavior.

Conflict of Interests

The authors declare that there is no conflict of interests regarding the publication of this paper.

Acknowledgments

This work has been supported by the National Science Foundation of China (Grant nos. 11322219, 11002124, 11202183, and 51107119) and the National High Technology Research and Development Program (863) of China (no. 2011AA11A101).

References

[1] P. G. Bruce, S. A. Freunberger, L. J. Hardwick, and J. Tarascon, "LigO 2 and LigS batteries with high energy storage," *Nature Materials*, vol. 11, no. 1, pp. 19–29, 2012.

[2] Y. Nomura, I. V. Anoshkin, C. Okuda et al., "Carbon nanotube/nanofibers and graphite hybrids for li-ion battery application," *Journal of Nanomaterials*, vol. 2014, Article ID 586241, 7 pages, 2014.

[3] J. Tarascon, "Is lithium the new gold?" *Nature Chemistry*, vol. 2, no. 6, p. 510, 2010.

[4] B. L. Ellis, W. R. M. Makahnouk, Y. Makimura, K. Toghill, and L. F. Nazar, "A multifunctional 3.5 V iron-based phosphate cathode for rechargeable batteries," *Nature Materials*, vol. 6, no. 10, pp. 749–753, 2007.

[5] J. Christensen, P. Albertus, R. S. Sanchez-Carrera et al., "A critical review of Li/air batteries," *Journal of the Electrochemical Society*, vol. 159, no. 2, pp. R1–R30, 2012.

[6] H. Wu, G. Chan, J. W. Choi et al., "Stable cycling of double-walled silicon nanotube battery anodes through solid-electrolyte interphase control," *Nature Nanotechnology*, vol. 7, no. 5, pp. 310–315, 2012.

[7] Y. Liu, N. S. Hudak, D. L. Huber, S. J. Limmer, J. P. Sullivan, and J. Y. Huang, "In situ transmission electron microscopy observation of pulverization of aluminum nanowires and evolution of the thin surface Al_2O_3 layers during lithiation-delithiation cycles," *Nano Letters*, vol. 11, no. 10, pp. 4188–4194, 2011.

[8] X. Lei, C. Wang, Z. H. Yi, Y. G. Liang, and J. T. Sun, "Effects of particle size on the electrochemical properties of aluminum powders as anode materials for lithium ion batteries," *Journal of Alloys and Compounds*, vol. 429, no. 1-2, pp. 311–315, 2007.

[9] Y. Hamon, T. Brousse, F. Jousse, P. Topart, P. Buvat, and D. M. Schleich, "Aluminum negative electrode in lithium ion batteries," *Journal of Power Sources*, vol. 97-98, pp. 185–187, 2001.

[10] D. Deng, M. G. Kim, J. Y. Lee, and J. Cho, "Green energy storage materials: Nanostructured TiO_2 and Sn-based anodes for lithium-ion batteries," *Energy and Environmental Science*, vol. 2, no. 8, pp. 818–837, 2009.

[11] S.-C. Chao, Y.-C. Yen, Y.-F. Song, Y.-M. Chen, H.-C. Wu, and N.-L. Wu, "A study on the interior microstructures of working Sn particle electrode of Li-ion batteries by in situ X-ray transmission microscopy," *Electrochemistry Communications*, vol. 12, no. 2, pp. 234–237, 2010.

[12] L. Baggetto and P. H. L. Notten, "Lithium-ion (De)insertion reaction of germanium thin-film electrodes: an electrochemical and in *situ* XRD study," *Journal of the Electrochemical Society*, vol. 156, no. 3, pp. A169–A175, 2009.

[13] L. Baggetto, J. K. Keum, J. F. Browning, and G. M. Veith, "Germanium as negative electrode material for sodium-ion batteries," *Electrochemistry Communications*, vol. 34, pp. 41–44, 2013.

[14] H. Yu, W. W. Zhang, S. Y. Lei, L. B. Lu, C. Sun, and Q. A. Huang, "Study on vibration behavior of doubly clamped silicon nanowires by molecular dynamics," *Journal of Nanomaterials*, vol. 2012, Article ID 342329, 5 pages, 2012.

[15] J. R. Szczech and S. Jin, "Nanostructured silicon for high capacity lithium battery anodes," *Energy and Environmental Science*, vol. 4, no. 1, pp. 56–72, 2011.

[16] X. H. Liu, L. Q. Zhang, L. Zhong et al., "Ultrafast electrochemical lithiation of individual Si nanowire anodes," *Nano Letters*, vol. 11, no. 6, pp. 2251–2258, 2011.

[17] Z. Wang, G. Xie, and L. Gao, "Electrochemical characterization of Li_4 Ti_5 O_{12}/C anode material prepared by starch-sol-assisted rheological phase method for Li-ion battery," *Journal of Nanomaterials*, vol. 2012, Article ID 876197, 7 pages, 2012.

[18] P. Balaya, H. Li, L. Kienle, and J. Maier, "Fully reversible homogeneous and heterogeneous Li storage in RuO_2 with high capacity," *Advanced Functional Materials*, vol. 13, no. 8, pp. 621–625, 2003.

[19] P. Poizot, S. Laruelle, S. Grugeon, L. Dupont, and J.-M. Tarascon, "Nano-sized transition-metal oxides as negative-electrode materials for lithium-ion batteries," *Nature*, vol. 407, no. 6803, pp. 496–499, 2000.

[20] C. K. Chan, H. L. Peng, G. Liu et al., "High-performance lithium battery anodes using silicon nanowires," *Nature Nanotechnology*, vol. 3, no. 1, pp. 31–35, 2008.

[21] Y. Jiang, Y. Sheng, X. Lan et al., "Mechanism and growth of flexible ZnO nanostructure arrays in a facile controlled way," *Journal of Nanomaterials*, vol. 2011, Article ID 473629, 12 pages, 2011.

[22] M. Park, G. Wang, Y. Kang, D. Wexler, S. Dou, and H. Liu, "Preparation and electrochemical properties of SnO_2 nanowires for application in lithium-ion batteries," *Angewandte Chemie*, vol. 46, no. 5, pp. 750–753, 2007.

[23] D. Wei, Y. Shen, M. Li et al., "Synthesis and characterization of single-crystalline SnO_2 nanowires," *Journal of Nanomaterials*, vol. 2013, Article ID 761498, 6 pages, 2013.

[24] K. M. Shaju, F. Jiao, A. Débart, and P. G. Bruce, "Mesoporous and nanowire Co_3O_4 as negative electrodes for rechargeable lithium batteries," *Physical Chemistry Chemical Physics*, vol. 9, no. 15, pp. 1837–1842, 2007.

[25] G. Armstrong, A. R. Armstrong, P. G. Bruce, P. Reale, and B. Scrosati, "TiO_2(B) nanowires as an improved anode material for lithium-ion batteries containing $LiFePO_4$ or $LiNi_{0.5}Mn_{1.5O4}$ cathodes and a polymer electrolyte," *Advanced Materials*, vol. 18, no. 19, pp. 2597–2600, 2006.

[26] A. M. Nie, J. B. Liu, Q. Q. Li et al., "Epitaxial TiO_2/SnO_2 core-shell heterostructure by atomic layer deposition," *Journal of Materials Chemistry*, vol. 22, no. 21, pp. 10665–10671, 2012.

[27] J. Y. Huang, L. Zhong, C. M. Wang et al., "*In situ* observation of the electrochemical lithiation of a single SnO_2 nanowire electrode," *Science*, vol. 330, no. 6010, pp. 1515–1520, 2010.

[28] J. W. Wang, X. H. Liu, S. X. Mao, and J. Y. Huang, "Microstructural evolution of tin nanoparticles during in situ sodium

insertion and extraction," *Nano Letters*, vol. 12, no. 11, pp. 5897–5902, 2012.

[29] M. D. Slater, D. Kim, E. Lee, and C. S. Johnson, "Sodium-ion batteries," *Advanced Functional Materials*, vol. 23, no. 8, pp. 947–958, 2013.

[30] X. Guan, L. Li, G. Li, Z. Fu, J. Zheng, and T. Yan, "Hierarchical CuO hollow microspheres: Controlled synthesis for enhanced lithium storage performance," *Journal of Alloys and Compounds*, vol. 509, no. 7, pp. 3367–3374, 2011.

[31] S. M. Abbas, S. T. Hussain, S. Ali et al., "One-pot synthesis of a composite of monodispersed CuO nanospheres on carbon nanotubes as anode material for lithium-ion batteries," *Journal of Alloys and Compounds*, vol. 574, pp. 221–226, 2013.

[32] S. K. Baek, K. R. Lee, and H. K. Cho, "Oxide p-n heterojunction of Cu_2O/ZnO nanowires and their photovoltaic performance," *Journal of Nanomaterials*, vol. 2013, Article ID 421371, 7 pages, 2013.

[33] S. Grugeon, S. Laruelle, R. Herrera-Urbina, L. Dupont, P. Poizot, and J. M. Tarascon, "Particle size effects on the electrochemical performance of copper oxides toward lithium," *Journal of the Electrochemical Society*, vol. 148, no. 4, pp. A285–A292, 2001.

[34] D. W. Zhang, C. H. Chen, J. Zhang, and F. Ren, "Novel electrochemical milling method to fabricate copper nanoparticles and nanofibers," *Chemistry of Materials*, vol. 17, no. 21, pp. 5242–5245, 2005.

[35] F. Ke, L. Huang, G. Wei et al., "One-step fabrication of CuO nanoribbons array electrode and its excellent lithium storage performance," *Electrochimica Acta*, vol. 54, no. 24, pp. 5825–5829, 2009.

[36] Y. Lee, I. Leu, C. Liao et al., "Fabrication and characterization of Cu_2O nanorod arrays and their electrochemical performance in Li-ion batteries," *Electrochemical and Solid-State Letters*, vol. 9, no. 4, pp. A207–A210, 2006.

[37] J. C. Park, J. Kim, H. Kwon, and H. Song, "Gram-scale synthesis of Cu_2O nanocubes and subsequent oxidation to CuO hollow nanostructures for Lithium-ion battery anode materials," *Advanced Materials*, vol. 21, no. 7, pp. 803–807, 2009.

[38] M. Farbod, N. M. Ghaffari, and I. Kazeminezhad, "Effect of growth parameters on photocatalytic properties of CuO nanowires fabricated by direct oxidation," *Materials Letters*, vol. 81, pp. 258–260, 2012.

[39] J. F. Xu, W. Ji, Z. X. Shen et al., "Raman spectra of CuO nanocrystals," *Journal of Raman Spectroscopy*, vol. 30, no. 5, pp. 413–415, 1999.

[40] P. F. Williams and S. P. S. Porto, "Symmetry-forbidden resonant Raman scattering in Cu_2O," *Physical Review B*, vol. 8, no. 4, pp. 1782–1785, 1973.

[41] A. E. Rakhshani, "Preparation, characteristics and photovoltaic properties of cuprous oxide-a review," *Solid State Electronics*, vol. 29, no. 1, pp. 7–17, 1986.

[42] A. Safaei, "Shape, structural, and energetic effects on the cohesive energy and melting point of nanocrystals," *The Journal of Physical Chemistry C*, vol. 114, no. 32, pp. 13482–13496, 2010.

[43] A. Safaei, M. Attarian Shandiz, S. Sanjabi, and Z. H. Barber, "Modeling the melting temperature of nanoparticles by an analytical approach," *Journal of Physical Chemistry C*, vol. 112, no. 1, pp. 99–105, 2008.

[44] Y. Xue, M. Zhao, and W. Lai, "Size-dependent phase transition temperatures of dispersed systems," *Physica B Condensed Matter*, vol. 408, no. 1, pp. 134–139, 2013.

[45] W. H. Qi and M. P. Wang, "Size and shape dependent melting temperature of metallic nanoparticles," *Materials Chemistry and Physics*, vol. 88, no. 2-3, pp. 280–284, 2004.

[46] K. K. Nanda, "Size-dependent melting of nanoparticles: hundred years of thermodynamic model," *Pramana*, vol. 72, no. 4, pp. 617–628, 2009.